Computers, Materials & Continua

Tech Science Press

DOI: 10.32604/cmc.2023.037297
Article

MSCNN-LSTM Model for Predicting Return Loss of the UHF Antenna in HF-UHF RFID Tag Antenna

Zhao Yang[1], Yuan Zhang[1], Lei Zhu[2,*], Lei Huang[1], Fangyu Hu[3], Yanping Du[1] and Xiaowei Li[1]

[1]School of Mechanical and Electrical Engineering, Beijing Institute of Graphic Communication, Beijing, 102600, China
[2]Postal Industry Technology R&D Center, Beijing Institute of Graphic Communication, Beijing, 102600, China
[3]Collage of Electronic Information and Automation, Civil Aviation University of China, Tianjin, 300300, China
*Corresponding Author: Lei Zhu. Email: zhulei@bigc.edu.cn
Received: 29 October 2022; Accepted: 23 December 2022

Abstract: High-frequency (HF) and ultrahigh-frequency (UHF) dual-band radio frequency identification (RFID) tags with both near-field and far-field communication can meet different application scenarios. However, it is time-consuming to calculate the return loss of a UHF antenna in a dual-band tag antenna using electromagnetic (EM) simulators. To overcome this, the present work proposes a model of a multi-scale convolutional neural network stacked with long and short-term memory (MSCNN-LSTM) for predicting the return loss of UHF antennas instead of EM simulators. In the proposed MSCNN-LSTM, the MSCNN has three branches, which include three convolution layers with different kernel sizes and numbers. Therefore, MSCNN can extract fine-grain localized information of the antenna and overall features. The LSTM can effectively learn the EM characteristics of different structures of the antenna to improve the prediction accuracy of the model. Experimental results show that the mean absolute error (0.0073), mean square error (0.00032), and root mean square error (0.01814) of the MSCNN-LSTM are better than those of other prediction methods. In predicting the return loss of 100 UHF antennas, compared with the simulation time of 4800 s for High Frequency Structure Simulator (HFSS), MSCNN-LSTM takes only 0.927519 s under the premise of ensuring prediction accuracy, significantly reducing the calculation time, which provides a basis for the rapid design of HF-UHF RFID tag antenna. Then MSCNN-LSTM is used to determine the dimensions of the UHF antenna quickly. The return loss of the designed dual-band RFID tag antenna is −58.76 and −22.63 dB at 13.56 and 915 MHz, respectively, achieving the desired goal.

Keywords: HF-UHF RFID tag antenna; multi-scale convolutional neural network; long-short term memory; return loss

1 Introduction

As an essential component of radio frequency identification (RFID) systems, RFID tags have the function of storing and transmitting the information. Compared with other tags, integrated high-frequency (HF)–ultrahigh-frequency (UHF) RFID tags are capable of both near-field (13.56 MHz) communication and far-field (860–960 MHz) operation, which have the unique advantage of meeting different application scenarios simultaneously [1,2], and their antenna designs are gradually receiving attention from the industry [1–4]. With the help of electromagnetic (EM) simulators to analyze the EM performance of the antenna has become an essential step in antenna design. Most simulators use numerical calculation methods to solve Maxwell equations for any given antenna, which has the advantage of high accuracy, there are also problems of complex computation and long solution time [5]. In addition, the non-linear relationship between the EM performance of RFID tag antennas and their physical dimensions leads to unclear optimization directions, requiring multiple simulation experiments to obtain the needed structures and dimensions. This not only increases the time cost of antenna design but may also face the problem of computational resources, such as memory bottlenecks.

Artificial neural network (ANN) is a viable solution to the above problems as it provides low computational cost solutions to complicated issues [5–7]. In recent years, related scholars have used ANN to construct the mapping relationship between RFID tag antenna dimensions and EM responses to predict the EM performance of the antenna, which saves time in calculating antenna performance and improves antenna design efficiency. For example, Li used back propagation (BP) network to predict the S-parameters of the printed dipole antenna, and the results had amplitude and phase errors of less than 0.09% [8]. Hong analyzed that the structural parameters of UHF RFID dipole tag antennas have sequential characteristics and used Bi-directional Long Short-Term Memory (BiLSTM) network to predict the return loss of the antennas. The BiLSTM had higher prediction accuracy compared with the non-sequential BP neural network and radial basis function (RBF) neural network [9]. Samson Daniel used ANN to optimize the performance of cavity-backed antenna loaded with slots for RFID applications [10]. However, there are comparatively few studies on ANN for EM performance prediction of RFID tag antennas, which have remarkable achievements in other antenna designs [11]. To mention a few, Sami Khafaga employed an improved LSTM to predict the bandwidth of a metamaterial antenna, and the predictions of the LSTM were superior compared to Multilayer Perceptron (MLP), K-Nearest Neighbors (KNN) and the basic LSTM [12]. Compared with LSTM and other networks, convolutional neural network (CNN) is more adept at extracting spatial features of antennas. Jacobs proposed a CNN for predicting resonant frequencies of dual-frequency pixelated microstrip antennas, the average relative errors of the predicted dual resonant frequencies are 0.13% and 0.22%, respectively, which were more accurate than the standard feedforward neural network [13]. Luo et al. proposed CNN that can be used for ultra-wideband antenna performance prediction, the inputs of the model were cross-sectional images or three views, and the outputs were the transfer function of the antenna [14].

The works described above achieve remarkable achievements, but still have certain limitations:

1) It is difficult for a one-sized convolution kernel to represent the overall information of the sample data as well as local features. In contrast, large kernels can extract the entire structure, while small kernels are better at extracting the fine-grain features [15].
2) CNN, LSTM, etc. cannot learn both temporal and spatial features simultaneously. CNN is highly efficient at learning spatial features while LSTM can effectively handle temporal features [16].

To overcome the limitations of single-size convolutional kernels, Roy proposed a multi-scale feature fused CNN that could effectively extract local fine-grained information at high frequencies and overall features at low frequencies in the electroencephalogram signals and dramatically enhanced the accuracy of the motor imagery classifier [15]. The integration of CNN and LSTM is an effective strategy to combine the advantages of both, and Rajesh Kanna et al. has successfully built efficient Intrusion Detection Systems based on this strategy [16,17]. When predicting antenna performance, both multi-scale CNN and LSTM are needed to extract the multiple features of the antenna. Thus, this paper proposes the multi-scale CNN stacked with long short-term memory (MSCNN-LSTM) model which can effectively predict the return loss of the UHF antennas in HF-UHF RFID tag antennas. The model can partly replace EM simulation software to improve the efficiency of HF-UHF RFID tag antenna design.

The core work of this paper is as follows:

1) The impedance of different structures of UHF antennas has been analyzed as it is a crucial factor affecting the return loss of the antenna.
2) The work designs a multi-branch and multi-scale CNN to learn fine-grain localized information of the antenna and overall features.
3) A stacked integration strategy of MSCNN and LSTM is adopted, which combines the respective advantages of both models to extract antenna features better and improve the prediction performance of the model.
4) The performance of CNN, LSTM, BiLSTM, and CNN-LSTM has been compared, and the results showed that the proposed MSCNN-LSTM accurately predicted the return loss and outperformed other models using the same dataset.
5) A single-chip integrated HF-UHF RFID tag antenna has been designed by the proposed MSCNN-LSTM.

The paper is organized as follows: Section 2 briefly introduces CNN and LSTM; The HF-UHF RFID tag antenna is described in Section 3; Section 4 details the features of the UHF antenna dimension data and the verification experiment of the proposed model MSCNN-LSTM. Finally, the conclusions of this paper and plans for future research are given in Section 5.

2 Theoretical Background

2.1 Convolutional Neural Network

Convolutional neural network (CNN) is a feedforward neural network proposed by LeCun et al. in 1998 [18]. The most central aspect of convolutional neural networks is the convolutional operation, which can be expressed as

$$y^{l+1} = a\left(\sum w^l * x^l + b^l\right) \tag{1}$$

where w^l, b^l are the weights and biases of layer l, respectively, and x^l denotes the inputs of layer l; a denotes the activation function.

MSCNN is a modified convolutional neural network. Unlike neural networks with a single convolutional kernel, MSCNN has different numbers and sizes of convolutional kernels distributed in multiple branches. The large convolution kernels can extract overall information, while small kernels are better at extracting the fine-grain features, thereby improving the feature expression ability of the network.

2.2 Long Short-Term Memory

Long short-term memory (LSTM) is an enhancement on the recurrent neural network (RNN), which largely overcomes the problems of gradient disappearance and gradient explosion by introducing memory units [19]. LSTM can retain critical features in input parameters for a long time, so it can effectively process a wide range of sequence data. As shown in Fig. 1, the inputs of the LSTM at the t-th update are the hidden information of the previous layer h_{t-1} and the memory unit c_{t-1} and the current input x_t, and the outputs are h_t and c_t. The structure of LSTM consists of three main gating units: the forget gate, the input gate, and the output gate.

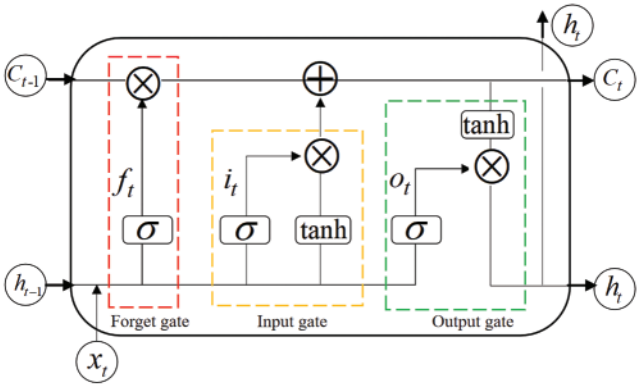

Figure 1: LSTM neuron internal structure

The forget gate is composed of the activation function σ, and its state update calculation formula is shown in Eq. (2). It decides if the memory unit c_{t-1} should be retained or thrown away.

$$f_t = \sigma(W_f \cdot [h_{t-1}, x_t] + b_f) \tag{2}$$

The input gate consists of activation functions σ and tanh, which is updated by Eq. (3), whose role is to regulate the degree to which the information $\widetilde{c}_t$ obtained by Eq. (4) is preserved to c_t. The update of c_t is completed by Eq. (5)

$$i_t = \sigma(W_i \cdot [h_{t-1}, x_t] + b_i) \tag{3}$$

$$\widetilde{c}_t = \tanh(W_c \cdot [h_{t-1}, x_t] + b_c) \tag{4}$$

$$c_t = f_t \otimes c_{t-1} + i_t \otimes \widetilde{c}_t \tag{5}$$

The output gate is composed of the activation functions σ and tanh, whose update equation is (6), and finally, the update of h_t is completed by Eq. (7).

$$o_t = \sigma(W_o \cdot [h_{t-1}, x_t] + b_o) \tag{6}$$

$$h_t = o_t \otimes \tanh(c_t) \tag{7}$$

In the above equations, W and b denote the weights and biases, respectively, and $\otimes$ denotes the product operation.

3 Design of HF-UHF RFID Tag Antenna

3.1 HF-UHF RFID Chip

The RFID tag chip in this paper is em|echo-V produced by EM Microelectronics, which is a dual frequency device that supports ISO/IEC15693, ISO/IEC18000-3 model 1, NFC Forum Type 5 Tag, ISO/IEC18000-63, EPC™ Gen2v2, and ISO/IEC29167-10. The electrical characteristics of the chip are shown in Table 1 [20].

Table 1: Electrical characteristics of the chip

Operating frequency	Resonance capacitor	Impedance
13.56 MHz	50 PF	——
915 MHz	——	17.6-j273 Ω

3.2 Design Goal of the HF-UHF RFID Tag Antenna

The energy source of the passive RFID tags is only the radio frequency energy transmitted by the RFID readers in the air. To improve the response distance of the tag, the antenna of the tag should have a good impedance match with the chip used, according to the maximum power transmission theory. The return loss (S_{11}) of the tag antenna port can effectively measure the degree of impedance matching between the antenna and chip. The S_{11} is computed by

$$S_{11} = 20 \lg \left(\frac{Z_a - Z_c^*}{Z_a + Z_c} \right) \tag{8}$$

where Z_a is the antenna input impedance, Z_c is the chip input impedance and Z_c^* is the conjugate value of chip impedance. According to the engineering requirements, this paper takes $S_{11} \leq -10$ dB as the design goal of the HF-UHF RFID tag antenna.

3.3 Structure of the HF-UHF RFID Tag Antenna

The simulation software used in this research is Ansoft High Frequency Structure Simulator (HFSS) 19.2; the computer hardware configurations are Intel (R) Core (TM) i7-9750HF CPU @ 2.60 GHz and 32G RAM.

The designed RFID tag antenna comprises a HF coil antenna and an UHF folded dipole antenna. Fig. 2 shows the structure of the HF coil antenna. The coil antenna distributes on both sides of the substrate in the form of a via-hole connection, and the winding direction is counterclockwise. The turn width and turn spacing of the coil antenna are represented by m and s. As shown in Fig. 3, the UHF antenna is a left-right symmetrical folded dipole antenna with a matching ring, and the end of the antenna are radiation patches; the overall structure of the HF-UHF RFID tag antenna is demonstrated in Fig. 3. The antenna builds on a polyethylene terephthalate film substrate of 2.7 relative permittivity and 0.075 mm of thickness, whose size varies with the d_{out} in the HF RFID tag antenna and the a_2 in the UHF RFID tag antenna.

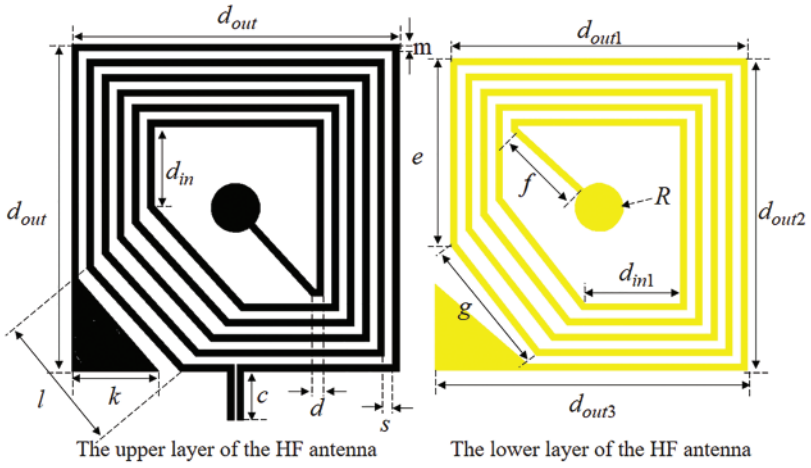

Figure 2: Structure of the HF RFID tag antenna

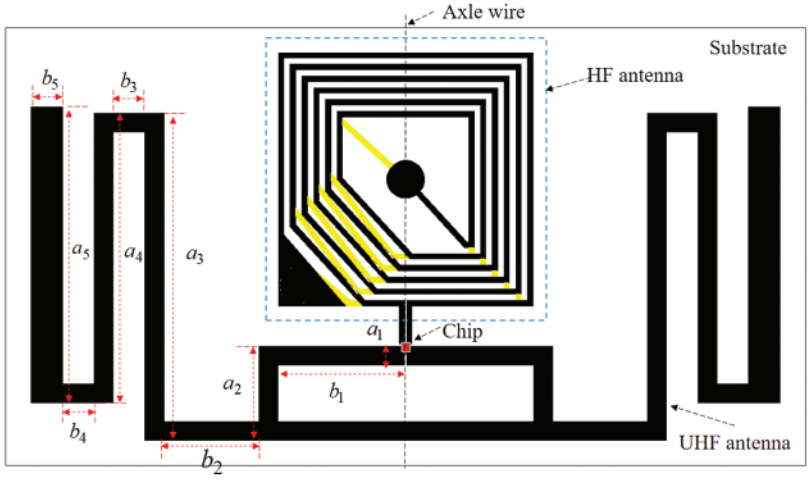

Figure 3: Structure of the HF-UHF tag antenna

Through experiments, it is found that the average simulation time of the HF RFID tag antenna is about 16 s, which is only 1/3 of the UHF antenna. This is because the mesh size of the finite element analysis method profile is related to the wavelength of the antenna, and the wavelength of the HF antenna is much larger than that of the UHF antenna. As a result, the HF antenna is relatively computationally small and the simulation time is comparatively short. As explained in [21], the HF RFID tag antenna has a significant impact on the impedance of the UHF RFID tag antenna, while the latter has a relatively small influence on the former. Therefore, this paper will obtain the structural dimensions of the HF coil antenna with the help of HFSS simulation software and design the UHF antenna based on it. Table 2 shows the dimensions of the HF antenna obtained from the simulation experiment. To prevent the UHF antenna from contacting the HF antenna, overlapping itself, or

exceeding the substrate, its dimensions must meet the following formulas:

$$\begin{cases} b_1 + b_2 > d_{out}/2 \\ a_2 > 2a_1 \\ a_3 < a_2 + c + d_{out} \\ a_4 < a_3 \\ a_5 \approx a_4 \end{cases} \tag{9}$$

Table 2: HF RFID tag antenna dimensions (unit: mm)

Parameter	Value	Parameter	Value	Parameter	Value
s	0.50	d_{in}	4.85	d	0.76
m	0.43	d_{in1}	10.89	e	11.50
d_{out}	20.12	k	5.37	f	5.65
d_{out1}	18.26	l	8.52	R	1.50
d_{out2}	18.19	g	8.58		
d_{out3}	18.19	c	3.00		

Table 3 shows the range of the structure parameters of the UHF antenna.

Table 3: Range of structure parameters of the UHF antenna (unit: mm)

Parameter	Range	Parameter	Range	Parameter	Range
a_1	[1, 2]	a_3	[24.5, 27.5]	a_5	[22, 25]
b_1	[9, 12]	b_3	[2, 4]	b_5	[1, 4]
a_2	[7, 10]	a_4	[21.5, 24.5]		
b_2	[6, 9]	b_4	[2, 5]		

4 MSCNN-LSTM Model Experiment

4.1 Data Preparation

Based on the initial structure of the HF-UHF RFID tag antenna shown in Fig. 3, this study used MATLAB to control the HFSS to randomly adjust the dimensions of the UHF antenna according to Table 3 to generate a total of 480 sets of antenna simulation data. Then, in the working frequency band (860 –960 MHz) of the UHF RFID tag antenna with a sampling interval of 4 MHz, the return loss of antennas at 21 frequency points were taken respectively, and 480 groups of antennas collected a total of 10,080 sample data.

4.2 Data Analysis

This section firstly introduces the structure of the UHF antenna, then shows the impact of each dimension change on UHF antenna impedance and explains the reason for changes from the principle, and finally infers the characteristics of UHF antenna dimension data and the relationship between the dimension and antenna return loss.

As shown in Fig. 4, the UHF antenna is a left-right symmetric structure with an impedance matching ring in the middle, a folded dipole connected to the matching ring, and radiating patches [22] at the end. a_1 represents the line width of the matching ring and the folded dipole, b_5 represents the width of the radiation patches. The dimensions of the structures to the left from the center axis of the UHF antenna are b_1, a_2, b_2, a_3, b_3, a_4, b_4 and a_5, respectively.

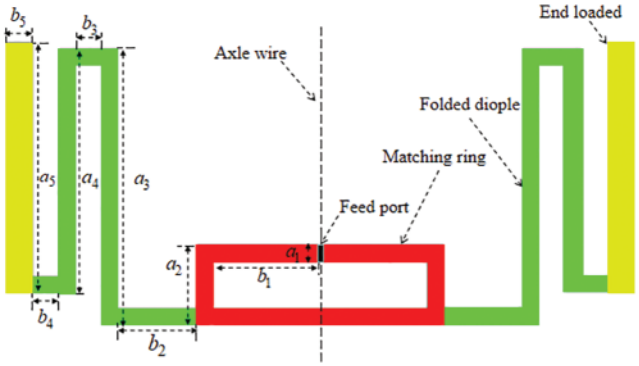

Figure 4: Structural division diagram of the UHF antenna

Fig. 5 presents the simulation result of UHF RFID tag antenna impedance changing with each dimension adjustment. The results show that the antenna impedance is related to each dimension, but there are differences in the degree of correlation. For example, b_1 and a_3 are increased by 3 mm in steps of 0.5 mm the former increases the antenna reactance and resistance by about 108 and 28 Ω, respectively; the latter can only change it by 17 and 4 Ω. The effect of the same dimension alteration on the resistance and reactance of the antenna is generally the same. Still, there are exceptions, and the b_4 is a case in point, when b_4 increases from 4 to 4.5 mm, the resistance of the antenna increases, and the reactance decreases. Finally, combined with Fig. 4, one can observe that the dimensions of the matching ring and the end radiation patches have a significant influence on the impedance of the UHF RFID tag antenna. This is because the ring structure can introduce inductance and capacitance, and the end-loading method can accumulate more charges and increase the equivalent capacitance of the tag antenna [22].

To sum up, we draw the following conclusions: the data of dimensions not only represents the dimensions of different structures of the antenna, reflecting the spatial features of the antenna but also implies the impedance characteristics of different structures, which determine the overall impedance of the antenna to a large extent.

As shown in Fig. 6, the return loss of the UHF RFID tag antenna varies with the antenna dimensions. According to the formula (8), UHF antenna return loss is related to the impedance of both the antenna and the chip, and the impedance of the chip at a specific frequency has been relatively fixed. Hence, it depends on the impedance of the antenna. Due to the impedance of the antenna is not linearly related to the dimensions, the return loss of the antenna is also a nonlinear mapping relationship with the dimensions.

4.3 MSCNN-LSTM Model

In this section, to obtain the non-linear mapping relationship between UHF antenna return loss and its dimensions, the MSCNN-LSTM model is established based on the spatial features of the

antenna simulation data and the impedance characteristics implied by it. The model of the MSCNN-LSTM is shown in the inset of Fig. 7.

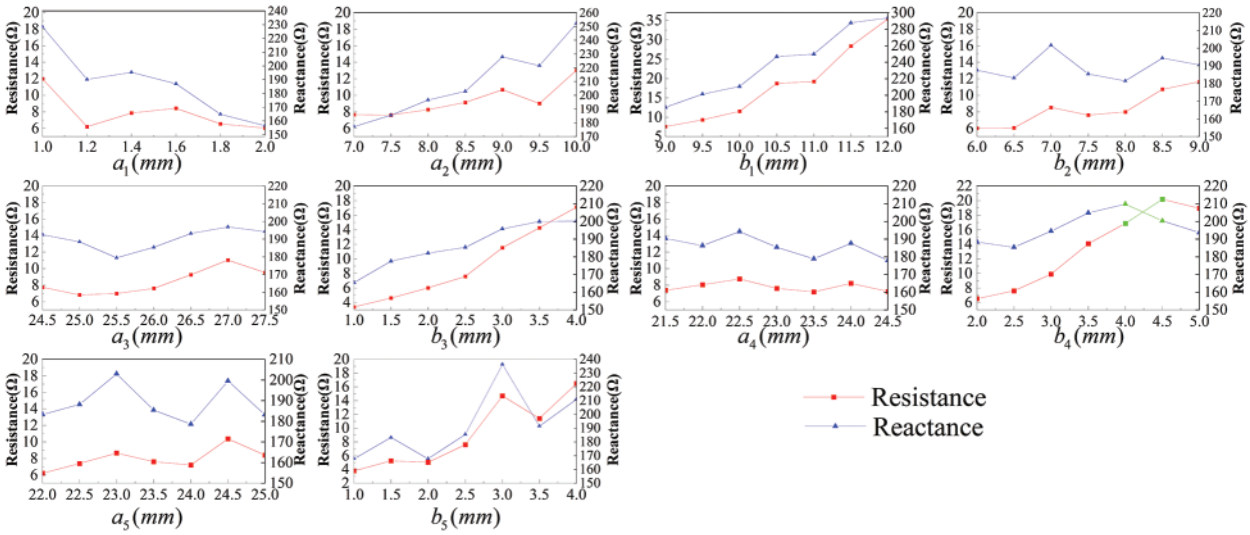

Figure 5: Simulation results of the UHF RFID tag antenna impedance variation with each dimension

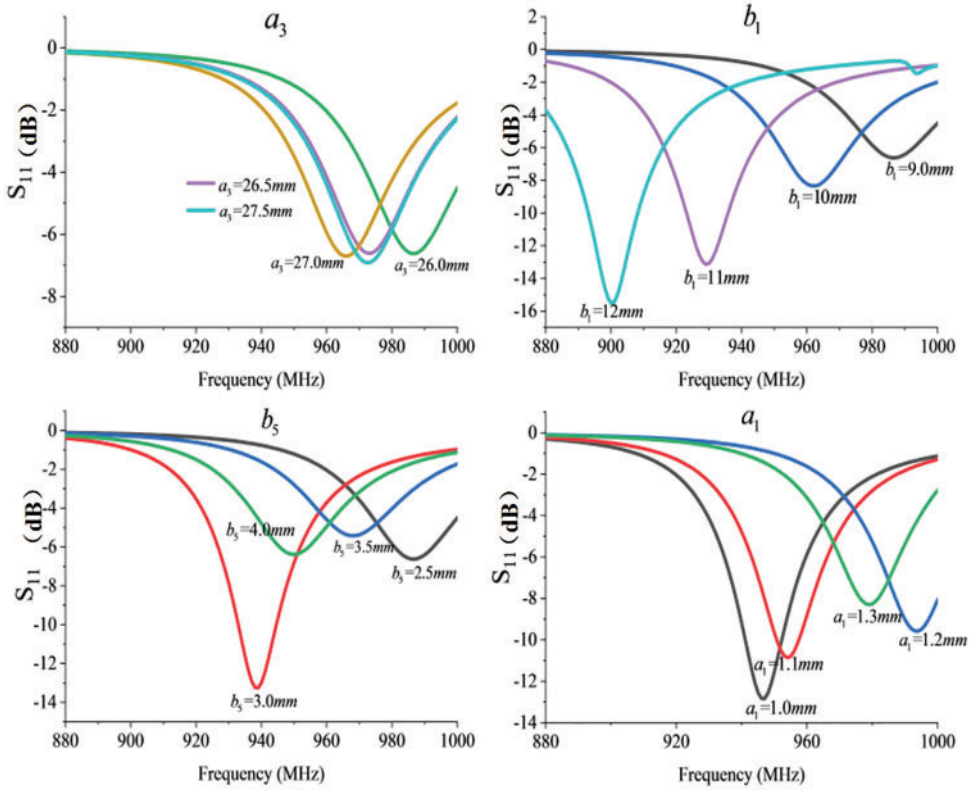

Figure 6: Simulation results of UHF RFID tag antenna return loss variation with each dimension

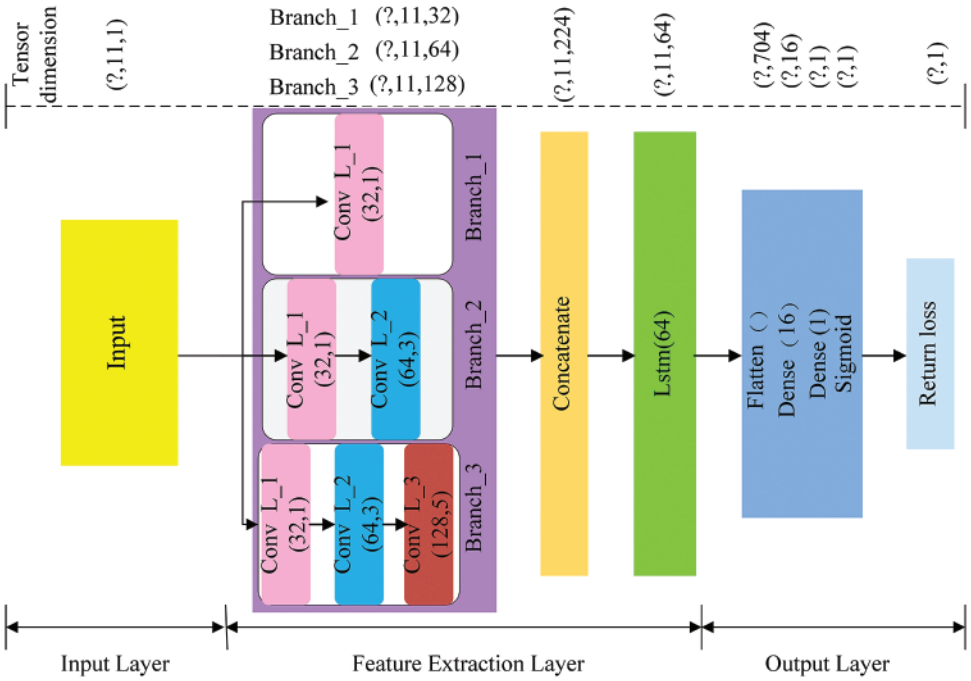

Figure 7: Structure of the MSCNN-LSTM

In the MSCNN-LSTM, ten structural parameters $(a_1, b_1, a_2, b_2, a_3, b_3, a_4, b_4, a_5, b_5)$ of the UHF antenna and one sampling frequency point are set as input, and the return loss of the antenna is set as output. The input shape is (?, 11, 1), "?" indicates the number of samples delivered per batch of training, which is taken as 10 in this article. 11 and 1 represent the length and dimension of the input, respectively. The feature extraction layer is divided into the MSCNN module, Concatenate module, and LSTM module. MSCNN has three branches, Branch_1 has one dimensional convolution layer_1 (Conv L_1), Branch_2 contains Conv L_1 and Conv L_2, and Branch_ 3 consists of three convolution layers, Conv L_1, Conv L_2, Conv L_3 in that order. The parameters of Conv L_1, Conv L_2 and Conv L_3 are (32, 1), (64, 3) and (128, 5), respectively. Where 32, 64, 128 represent the number of convolution kernels, and 1, 3, and 5 are the size of the kernels. Conv L_1 uses relatively small convolution kernels, which can automatically extract fine-grain features of the antenna. Conv L_2 has a medium-sized kernel to extract the relatively coarse grain features of the antenna. Whereas, Conv L_3 extracts the overall features of the antenna, hence uses the larger kernel [15]. In addition, as the convolution depth increases and the size of the convolution kernels grows, more feature information is accumulated, and we increase the number of convolution kernels in the later convolution layers to fully extract the feature information. In each convolutional layer, the stride is 1, the padding is SAME, and the activation function is rectified linear unit (ReLU) which can improve the training speed of neural networks. Passing through Branch_1, the tensor dimension of the input data becomes (?, 11, 32). In Branch_2, the input data passes through Conv L_1and then Conv L_2, and the dimension of the tensor becomes (? 11, 64). The input data passes through the three convolutional layers in Branch_3 in turn, and the tensor dimension is changed to (? 11, 128).

The Concatenate module connects the features from the three branches to obtain broader feature information. The output shape of Concatenate module is (?, 11, 224).

Long-term memory retention is one of the main advantages of LSTM. As demonstrated in [12], the LSTM also performs well in the prediction of antenna performance. This paper input the dimension data into the model in the order of the structure of the UHF RFID tag antenna so that the LSTM with 64 units can fully extract the EM characteristics of the antenna, after which the feature information is flattened into a vector of 704 by the flatten layer. The feature information then enters a fully connected layer consisting of two dense layers. Two dense layers can improve the accuracy of the prediction results. Finally, the last feature information is used to predict the return loss of the UHF antenna via the Sigmoid layer.

4.4 Training of MSCNN-LSTM Model

This paper built related algorithm models based on the deep learning framework TensorFlow.

At the beginning of model training, we normalized the sample data to [0, 1] to improve the efficiency of model training [23]. These 10080 samples were then randomly divided into training and testing sets in an 8:2 ratio. The parameters of the model were optimized using the Adam optimizer during the model training process, with the initial learning rate set to 0.001 and the number of iterations trained to 100. The top part of Fig. 7 shows the change in tensor dimension after the data has gone through each module.

4.5 Performance Analysis of MSCNN-LSTM

Four models of CNN, LSTM, CNN-LSTM and BiLSTM [9] with the same training parameters as the MSCNN-LSTM were built to verify the prediction ability of the MSCNN-LSTM model on the return loss of UHF antenna in HF-UHF RFID tag antenna. The prediction performance of each model was quantified by using the mean absolute error (MAE), mean square error (MSE), and root mean square error (RMSE) evaluation metrics. The evaluation metric is calculated as follows:

$$MAE = \frac{1}{n}\sum_{i=1}^{n} \left| y_{pre_i} - y_{true_i} \right| \tag{10}$$

$$MSE = \frac{1}{n}\sum_{i=1}^{n} \left(y_{pre_i} - y_{true_i} \right)^2 \tag{11}$$

$$RMSE = \sqrt{\frac{1}{n}\sum_{i=1}^{n} \left(y_{pre_i} - y_{true_i} \right)^2} \tag{12}$$

Table 4 shows the prediction errors of MSCNN-LSTM, CNN-LSTM, LSTM, CNN, and BiLSTM [9] models in the test set and the time consumption comparison with HFSS for calculating the return loss of 100 UHF antennas. The smaller the value of each evaluation index of the model, the closer the predicted value of return loss is to the simulated value of HFSS, and the superior prediction performance of the model. As shown in Table 4, the MAE, MSE, and RMSE of MSCNN-LSTM are 0.0073, 0.00032, and 0.01814 are smaller than the evaluation results of other models, indicating that the MSCNN-LSTM model proposed in this paper is superior to CNN-LSTM, LSTM, CNN, and BiLSTM [9] in UHF antenna return loss prediction. The evaluation indexes of MSCNN-LSTM are better than those of CNN-LSTM, reflecting the comprehensiveness and superiority of MSCNN in extracting antenna spatial features. The error of CNN-LSTM is smaller than that of LSTM and CNN, which means that combining CNN and LSTM can make up for the shortcomings of each and give full play to the advantages of both to improve the accuracy for predicting antenna performance. It can also be found that the prediction accuracy of LSTM is slightly higher than that of CNN, which is related to the electromagnetic characteristics of the different structures of the antenna, and it is

difficult to reflect this intrinsic difference from the shape of the antenna alone. Table 4 shows that the BiLSTM [9] is marginally more precise than the LSTM, but it is not as powerful as the combination of the LSTM and CNN.

Table 4: Error of each model and comparison with HFSS time consumption

Model	MAE	MSE	RMSE	Time spent/s
CNN	0.0352	0.00289	0.05378	0.192527
LSTM	0.0144	0.00065	0.02563	0.682110
BiLSTM [9]	0.0130	0.00056	0.02382	0.612393
CNN-LSTM	0.0120	0.00056	0.02373	0.744010
MSCNN-LSTM	0.0073	0.00032	0.01814	0.927519
HFSS	——	——	——	4800

On the other hand, from the perspective of computation time, MSCNN-LSTM and other comparative models can evaluate the return loss of 100 UHF antennas in less than 1 s, while HFSS requires 4800 s. MSCNN-LSTM is relatively complex in terms of network structure, causing it to fall behind in terms of time consumption. Still the difference of less than 1 s between the models is entirely negligible compared to the simulation time of HFSS.

Fig. 8 shows the prediction performance of the MSCNN-LSTM model in partial test sets, the black dash-dot line represents the simulated values of the return loss of different antennas at different frequencies, and the red dash-dot line indicates the predicted values. In Fig. 8, the black simulation value distribution is irregular. However, each red prediction value is still very close to the black simulation value, which proves that the model can effectively predict the return loss of the UHF antenna.

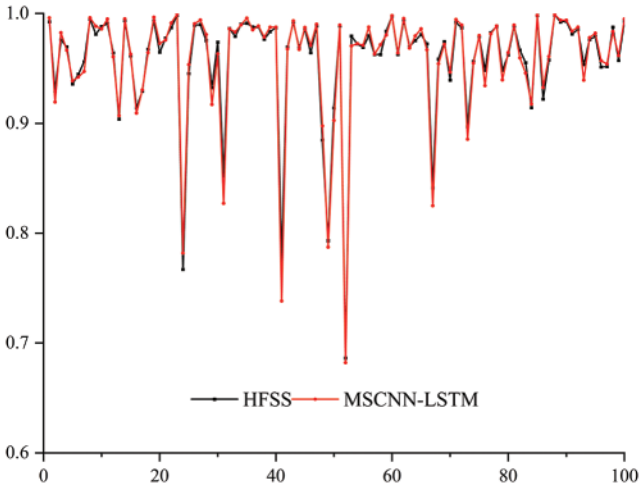

Figure 8: Example of MSCNN predictions

The prediction results of each model for some UHF antennas that are not in the sample data demonstrated in Fig. 9, from which it can be found that the predicted values of MSCNN-LSTM are closer to the simulation value of HFSS, and the prediction performances surpass that of CNN-LSTM

and LSTM. Moreover, the accuracy of the MSCNN-LSTM in predicting the return loss near the resonance point is also improved compared to the literature [24], which is invaluable as the return loss at the impedance matching point of the RFID tag antenna usually drops dramatically, making it more difficult to predict.

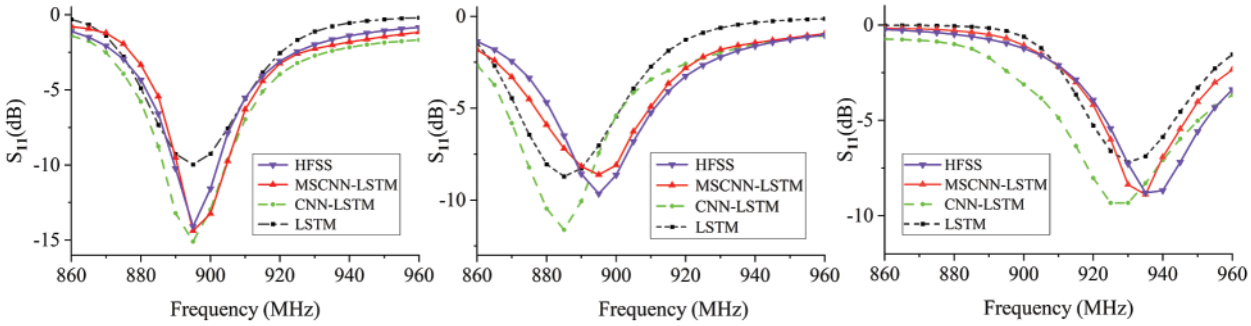

Figure 9: Prediction effect of each model for UHF antennas

Combining Table 4, Figs. 8 and 9, it can be concluded that compared to HFSS simulation calculation, MSCNN-LSTM greatly reduces the computational time consumption with guaranteed prediction accuracy, providing a basis for the fast design of HF-UHF RFID tag antennas.

4.6 Determine the Antenna Dimensions of the HF–UHF RFID Tag

Table 5 shows a set of UHF antenna dimensions with good return loss at 915 MHz predicted using the MSCNN-LSTM. Combined with the dimensions of the HF antenna in Section 3, the dimensions of the HF-UHF RFID tag antenna were determined in this paper.

Table 5: UHF antenna structure dimensions (unit: mm)

Parameter	Value	Parameter	Value	Parameter	Value
a_1	1.4	a_3	25.8	a_5	24.6
b_1	9.6	b_3	2.3	b_5	2.7
a_2	9.3	a_4	24.1		
b_2	7	b_4	3.1		

Fig. 10 depicts the return loss of the designed HF-UHF RFID tag antenna. In Fig. 10, the return loss of the HF antenna at 13.56 MHz is −58.76 dB, and the return loss of the UHF antenna at 915 MHz is −22.63 dB, both of which are less than −10 dB, indicating that the antenna and the chip have good impedance matching. The design goal of the HF UHF RFID tag antenna has been achieved.

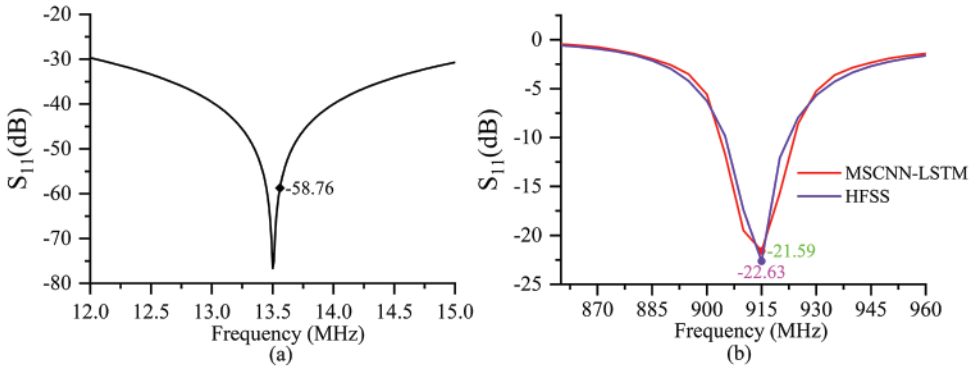

Figure 10: (a) Return loss of HF antenna; (b) Return loss of UHF antenna

5 Conclusion

In this paper, a new deep learning framework called MSCNN-LSTM has been proposed for predicting the return loss of the UHF antenna in HF-UHF RFID tag antenna, which is comprised of multi-scale convolutional neural network and long short-term memory. The model combines the advantages of both MSCNN and LSTM networks, which can extract fine-grain localized information of the antenna as well as overall spatial features and learn the EM characteristics of the different structures of the antenna. The proposed MSCNN-LSTM was validated using simulated data of UHF antennas in HF-UHF RFID antennas and compared with other prediction methods. Experimental results showed that the MAE (0.0073), MSE (0.00032), and RMSE (0.01814) of MSCNN-LSTM were the smallest compared to CNN, LSTM, BiLSTM, and CNN-LSTM. MSCNN-LSTM was significantly more accurate in predicting the return loss of UHF antennas than the previous four. In terms of computational time consumption, MSCNN-LSTM had a significant advantage over the simulation time of HFSS. The return loss of the dual-band RFID tag antenna designed with the assistance of MSCNN-LSTM was −58.76 and −22.63 dB at 13.56 and 915 MHz, respectively, which was a good conjugate match with the chip used and achieved the desired goal. In future research, we will try to refine the structure of the MSCNN-LSTM and apply it to the design of other antennas.

Acknowledgement: We sincerely thank our colleagues who contributed to the article but were not mentioned.

Funding Statement: The research work is carried out under the Beijing Natural Science Foundation-Beijing Education Commission Joint Project (KZ202210015020), Discipline Construction and Postgraduate Education Project of BIGC (No. 21090122005) and BIGC Project (Ee202204).

Conflicts of Interest: The authors declare that they have no conflicts of interest to report regarding the present study.

References

[1] H. S. Farahani, B. Rezaee, M. Gadringer, W. Bosch, L. Zoscher *et al.,* "A miniaturized HF/UHF dual-band RFID tag antenna," in *2021 IEEE Int. Symp. on Antennas and Propagation and USNC-URSI Radio Science Meeting (APS/URSI)*, Singapore, pp. 383–384, 2021.

[2] A. Sakonkanapong and C. Phongcharoenpanich, "Near-field HF-RFID and CMA-based circularly polarized far-field UHF-RFID integrated tag antenna," *International Journal of Antennas and Propagation*, vol. 2020, pp. 1–15, 2020.
[3] P. Wang, L. Dong, H. Wang, G. Li, Y. Di *et al.,* "Passive wireless dual-tag UHF RFID sensor system for surface crack monitoring," *Sensors (Basel)*, vol. 21, no. 3, pp. 1–16, 2021.
[4] N. Ha-Van and C. Seo, "A single-feeding port HF-UHF dual-band RFID tag antenna," *Journal of Electromagnetic Engineering and Science*, vol. 17, no. 4, pp. 233–237, 2017.
[5] A. I. Hammoodi, M. Milanova and H. Khaleel, "Design of flexible antenna for UWB wireless applications using ANN," in *2017 Int. Conf. on Computational Science and Computational Intelligence (CSCI)*, USA, pp. 751–754, 2017.
[6] A. Chandio, G. Gui, T. Kumar, I. Ullah, R. Ranjbarzadeh *et al.,* "Precise single-stage detector," arXiv preprint arXiv:2210.04252, pp. 1–33, 2022.
[7] W. Khan, K. Raj, T. Kumar, A. M. Roy and B. Luo, "Introducing urdu digits dataset with demonstration of an efficient and robust noisy decoder-based pseudo example generator," *Symmetry*, vol. 14, no. 10, pp. 1–15, 2022.
[8] X. Li, J. Gao and G. Boeck, "Printed dipole antenna design using artificial neural network modeling for RFID application," *International Journal of RF and Microwave Computer-Aided Engineering*, vol. 16, no. 6, pp. 607–611, 2006.
[9] T. Hong, Z. He, C. Wang, J. Chen and J. Zhou, "Fast multi-objective RFID tag antenna design based on BiLSTM surrogate model," *Journal of Microwaves*, vol. 37, no. 1, pp. 21–27, 2021.
[10] R. S. Daniel, "Multiband substrate integrated waveguide antenna loaded with slots using artificial neural network," *International Journal of RF and Microwave Computer-Aided Engineering*, vol. 32, no. 10, pp. 1–12, 2022.
[11] A. Katkevičius, D. Plonis, R. Damaševičius and R. Maskeliūnas, "Trends of microwave devices design based on artificial neural networks: A review," *Electronics*, vol. 11, no. 15, pp. 1–21, 2022.
[12] D. Sami Khafaga, A. Ali Alhussan, E. -S. M. El-kenawy, A. Ibrahim, S. H. Abd Elkhalik *et al.,* "Improved prediction of metamaterial antenna bandwidth using adaptive optimization of LSTM," *Computers, Materials & Continua*, vol. 73, no. 1, pp. 865–881, 2022.
[13] J. P. Jacobs, "Accurate modeling by convolutional neural-network regression of resonant frequencies of dual-band pixelated microstrip antenna," *IEEE Antennas and Wireless Propagation Letters*, vol. 20, no. 12, pp. 2417–2421, 2021.
[14] H. -Y. Luo, Y. Hong, Y. -H. Lv and W. Shao, "Parametric modeling of UWB antennas using convolutional neural networks," in *2020 IEEE Int. Symp. on Antennas and Propagation and North American Radio Science Meeting*, Montreal, Quebec, Canada, pp. 2055–2056, 2020.
[15] A. M. Roy, "Adaptive transfer learning-based multiscale feature fused deep convolutional neural network for EEG MI multiclassification in brain–computer interface," *Engineering Applications of Artificial Intelligence*, vol. 116, pp. 1–17, 2022.
[16] P. R. Kanna and P. Santhi, "Hybrid intrusion detection using mapreduce based black widow optimized convolutional long short-term memory neural networks," *Expert Systems with Applications*, vol. 194, pp. 116545, 2022.
[17] P. Rajesh Kanna and P. Santhi, "Unified deep learning approach for efficient intrusion detection system using integrated spatial–temporal features," *Knowledge-Based Systems*, vol. 226, pp. 1–12, 2021.
[18] Y. LeCun, L. Bottou, Y. Bengio and P. Haffner, "Gradient-based learning applied to document recognition," *Proceedings of the IEEE*, vol. 86, no. 11, pp. 2278–2324, 1998.
[19] A. S. Navathe, M. Mugiishi and E. J. Emanuel, "Population-based primary care payment system in Hawaii-reply," *JAMA*, vol. 322, no. 21, pp. 2136–2137, 2019.
[20] https://www.emmicroelectronic.com/product/nfc-high-frequency-ics/em-echo-v
[21] Z. Yang, Y. Zhang, L. Zhu, L. Shen, Y. Du *et al.,* "Design of a single chip HF-UHF dual-band RFID tag antenna," in *Interdisciplinary Research for Printing and Packaging*, Springer, Singapore, pp. 301–305, 2022.

[22] N. Faudzi, M. Ali, I. Ismail, H. Jumaat and N. Sukaimi, "A compact dipole UHF-RFID tag antenna," in *2013 IEEE Int. RF and Microwave Conf. (RFM)*, CA, USA, pp. 314–317, 2013.

[23] S. Ioffe and C. Szegedy, "Batch normalization: Accelerating deep network training by reducing internal covariate shift," in *Int. Conf. on Machine Learning*, PMLR, pp. 448–456, 2015.

[24] Y. -F. Liu, L. Peng and W. Shao, "An efficient knowledge-based artificial neural network for the design of circularly polarized 3-D-printed lens antenna," *IEEE Transactions on Antennas and Propagation*, vol. 70, no. 7, pp. 5007–5014, 2022.